Talanta 215 (2020) 120904

Contents lists available at ScienceDirect

Talanta

journal homepage: www.elsevier.com/locate/talanta

*Legionella p*neumophila sg1-sensing signal enhancement using a novel electrochemical immunosensor in dynamic detection mode

Ahlem Laribi[a,b,*], Séverine Allegra[a], Mina Souiri[b], Ridha Mzoughi[c], Ali Othmane[b], Françoise Girardot[a]

[a] Environments, Territories, Societies (EVS) Lab, Mixed Research Unit (Jean Monnet University - French National Centre for Scientific Research) 5600, University of Lyon, F42023, France

[b] Laboratory of Advanced Materials and Interfaces, Faculty of Medicine, University of Monastir, 5019, Monastir, Tunisia

[c] Regional Laboratory of Hygiene, University Hospital Farhat Hached, 4000 Sousse, Tunisia and Laboratory of Analysis Treatment and Valorization of Pollutants and Products, Faculty of Pharmacy, 5000, Monastir, Tunisia

ARTICLE INFO

Keywords:
Legionella pneumophila
Electrochemical detection
Microfluidic device
Immunosensor

ABSTRACT

This work presents a comparison between static and dynamic modes of biosensing using a novel microfluidic assay for continuous and quantitative detection of *Legionella pneumophila* sg1 in artificial water samples. A self-assembled monolayer of 16-amino-1-hexadecanethiol (16-AHT) was covalently linked to a gold substrate, and the resulting modified surface was used to immobilize an anti-*Legionella pneumophila* monoclonal antibody (mAb). The modified surfaces formed during the biosensor functionalization steps were characterized using electrochemical measurements and microscopic imaging techniques. Under static conditions, the biosensor exhibited a wide linear response range from 10 to 10^8 CFU/mL and a detection limit of 10 CFU/mL. Using a microfluidic system, the biosensor responses exhibited a linear relationship for low bacterial concentrations ranging from 10 to 10^3 CFU/mL under dynamic conditions and an enhancement of sensing signals by a factor of 4.5 compared to the sensing signals obtained under static conditions with the same biosensor for the detection of *Legionella* cells in artificially contaminated samples.

1. Introduction

Legionella pneumophila is the main vector of Legionnaires' disease, a type of pneumonia that can be fatal in humans. Indeed, inhalation of contaminated aerosols can cause bilateral pneumonia [1]. It has been reported that 9% of domestic cases are fatal [2], reaching between 25 and 48% for nosocomial cases in the USA [3]. In France, there was a 75% increase in the number of recorded incidences in 2018 compared to the previous year [4].

Legionella bacteria are found in natural aquatic environments and wet soils [5]. They are known to colonize artificial human-made aquatic ecosystems such as hot water distribution systems, air conditioning systems, and air-cooling towers, thereby giving rise to severe outbreaks of pneumonia [6,7]. Approximately 28 sources of sporadic cases involving potable water, hot springs, humidifiers, water fountains, and medical respiratory equipment have been identified [8]. Therefore, any water system that generates aerosols from water should be considered at-risk [9,10]. For this reason, effective monitoring of water systems is critical. However, current standardized detection and enumeration methods (ISO 11731 and AFNOR T90 431 for cultures and ISO 12869 and AFNOR T90 471 for quantitative PCR) suffer from limitations that hinder proper and timely diagnosis [7].

Analysis by culture takes up to 10 days and the recovery of *Legionella* is not optimal due to the acid treatment and concentration stage [11]. Viable but nonculturable cells (VBNC), which are compromised cells characterized by a loss of culturability, are not detected using cultures [12], whereas it has been demonstrated that they are nonetheless still able to infect amoebae and human macrophages [13,14]. Several studies have demonstrated that VBNC forms are systematically present in potable water sources due to the presence of disinfection products and their low levels of nutrients [14,15].

Quantitative PCR (qPCR) is fast and easy to implement. However, it is limited by its inability to discriminate between dead and live cells, not to mention the need for specialized knowledge and experience to operate the equipment.

Furthermore, both techniques require harvesting of water samples

* Corresponding author. Environments, Territories, Societies (EVS) Lab, Mixed Research Unit (Jean Monnet University - French National Centre for Scientific Research) 5600, University of Lyon, F42023, Frasnce.

E-mail address: ahlem.laribi@etu.univ-st-etienne.fr (A. Laribi).

https://doi.org/10.1016/j.talanta.2020.120904
Received 24 November 2019; Received in revised form 3 March 2020; Accepted 5 March 2020
Available online 10 March 2020
0039-9140/

and further lab-based analyses.

Contaminated water systems are mainly disinfected using chlorine or heat treatment by exposure to high temperatures (70 °C for 30 min). It has been shown that up to 25% of *Legionella* bacteria can survive after such a heat treatment, and they are able to regrow after a few months [16]. In light of the reasons outlined above, there is hence a clear need to develop fast, sensitive, portable, and easy-to-use devices to achieve continuous monitoring of *Legionella* that can be applied directly to the water system.

Biosensors are considered to be a valuable alternative in this field. However, despite their remarkable sensitivity and biological compatibility, only a small number of practical studies have investigated the use of immunosensors to address this issue.

In this context, an optical fibre sensor based on surface plasmon resonance has been reported to provide a limit of detection of approximately 10 CFU/mL [17]. A similar sensitivity can be obtained using an electrochemical impedance spectroscopy immunosensor [18], and this LOD is considered to be the lowest detected concentration. For instance, Li et al. [19] and Lei et al. [20] reached LOD values of 10^2 Cells/mL and 10^5 CFU/mL, respectively, using an impedimetric immunosensor to detect *Legionella pneumophila*. Using an amperometric magnetic immunoassay assay for *Legionella pneumophila* detection, Martini et al. reported a LOD of 10^4 CFU/mL, with the possibility of detecting *Legionella* cells at 10 CFU/mL after a preconcentration step [21].

Using surface plasmon resonance technology for *Legionella pneumophila* detection, Enrico et al. [22] and Foudeh et al. [23] reported LOD values of ~10^4 CFU/mL. More recently, Aziziyan et al. have used the negative zeta potential, enhanced by decorating *Legionella pneumophila* with negatively charged sodium dodecyl sulphate molecules, to achieve a detection limit of 10^3 CFU/mL [24]. Despite their high sensitivities, these methods require specific equipment, as well as the necessary skills and expertise to properly interpret the sensing data. By using genosensors, which allow the detection of a specific DNA sequence, several authors have been able to achieve very low quantification limits of 10^{-21} M [25] and 10^{-14} M [26]. Nevertheless, despite their high sensitivities, genosensors cannot be used to detect and quantify live bacterial cells in water samples.

In light of these various reasons, in this study, we investigated a new version of a microfluidic immunosensor based on a combination of biosensor technology for *Legionella* detection and microfluidic systems.

2. Experimental

2.1. Chemicals and reagents

Phosphate-buffered saline (PBS) (0.01 M, pH 7.4), sulphuric acid (95–97%), bovine serum albumin (BSA, ≥ 96%), hydrogen peroxide solution (H_2O_2, 30%), acetone, N-(3-Dimethylaminopropyl)-N′-ethylcarbodiimide hydrochloride (EDC), N-Hydroxysuccinimide (NHS), and 16-Amino-1-hexadecanethiol hydrochloride (16-AHT) were purchased from Sigma-Aldrich.

BupH™ MES Buffered Saline Packs (MES) were purchased from Thermo Fisher Scientific and ethanol (99.8%) was purchased from Fluka.

Monoclonal mouse anti-*Legionella* antibody Dp-Lp1-O2 provided by Microbiodetection SARL (Commercy, France) was stored frozen, and three standard solutions were prepared daily at 0.1, 0.05, and 0.01 mg/mL in HEPES-buffered saline (HBS) composed of 10 mM HEPES and 150 mM NaCl.

All chemicals were analytical grade and were used without further purification.

2.2. Bacterial strain

A *Legionella pneumophila* sg1-GFP strain (Lp1-008-GFP) previously validated [27] for the expression of green fluorescent protein (GFP) was cultured on buffered charcoal yeast extract agar (BCYEα medium) containing chloramphenicol and incubated at 37 °C for 72 h to obtain exponential phase forms. All of the bacterial samples were freshly prepared by resuspension of colonies in an appropriate volume of PBS (Dulbecco's Phosphate-Buffered Solution, Sigma, France). An optical density (OD) of 0.2 at 600 nm (Biomate TM3; Avantec, Illkirch, France) was taken as a reference for the initial suspension containing 10^8 CFU/mL. Ten-fold serial dilutions from 10 to 10^8 CFU/mL were prepared and used to study the biosensing performance in both static and dynamic detection mode. The concentration of each independent initial suspension was determined by twice plating 100 µL aliquots of 10^2 and 10^3 dilutions on BCYE agar medium. The *Legionella* colonies were counted using a Scan 1200 enumerating system-Interscience, after 72 h at 37 °C.

2.3. Apparatus

All of the electrochemical measurements were performed at pH 7.4 in a 0.01 M PBS solution containing 0.1 M KCl and 10 mM $[Fe(CN)_6]^{3-/4-}$ (the reaction is controlled by diffusion of the ferri/ferrocyanide system as a redox probe) using a portable bipotentiostat (Metrohm, France SAS). Cyclic voltammograms (CV) were recorded at a scan range from - 0.4 to + 0.6 V with a scan rate of 0.05 V/s. Square-wave voltammograms (SWV) were recorded from - 0.3 to + 0.5 V using the following parameters: a frequency of 5 Hz, a pulse amplitude of 0.002 V, and a scan rate of 0.05 V s^{-1}. To guarantee reproducibility, each experiment was carried out independently at least three times using three different SPEs. The Drop View 8400 software plots the results as SWV and CV curves. The experiments were performed using a three-electrode system with Au as the working electrode, Pt as the auxiliary electrode, and Ag as the reference electrode.

Validation of functionalization was carried out by electrochemical measurements after each functionalization step and by visualization of the morphological changes using scanning electron microscopy (SEM, Nova Nanosem FEI 200, accelerating voltage 20 kV), and atomic force microscopy (AFM, Agilent 5500 LS instrument, Les Ulis, France). Before being observed by AFM, the SPEs were rinsed using ultrapure water and dried under nitrogen (N_2) to prevent the formation of salt crystals. The images were processed using GWIDDION software (version 2.52). The root mean square (RMS) was used to characterize the surface roughness in terms of the irregularity and height distribution. Confocal laser scanning microscopy (CLSM) images were obtained using a TCS-SP2 inverted confocal scanning laser microscope (LEICA Microsystems, Nanterre, France), with argon as an excitation source (488 nm).

2.4. Fabrication of the biosensor

Screen-printed electrodes (SPEs), were purchased from Metrohm, France. The SPEs were first rinsed with an acetone and ethanol solution to remove physically adsorbed contaminants. The working area (4-mm diameter) was then immersed for 1 min in a fresh piranha solution of 3:1 (v/v) 98% H_2SO_4/30% H_2O_2 using all the necessary safety procedures. The SPEs were then rinsed extensively with ultrapure water several times and finally dried in air.

Once cleaned, the SPEs were immersed in a solution of 2 mM 16-amino-1-hexadecanethiol 16-AHT in 99.8% ethanol for 24 h in the dark at 4 °C to form self-assembled monolayers.

The carboxyl groups located on the crystallizable fragment of the heavy chains of the anti-*L. pneumophila* monoclonal antibody (mAb) were activated using EDC (dissolved in MES) as described by Ref. [28,29].

Despite its importance for the biosensing performance [28–30], it is still difficult to ensure the orientation of the antibody during the activation process.

According to the literature, the use of EDC [29,31] or EDC/N-hydroxysulfosuccinimide (NHS) [32,33] or EDC with Sulfo-NHS [34] enables chemical activation of the carboxyl groups. Thus, the antibody

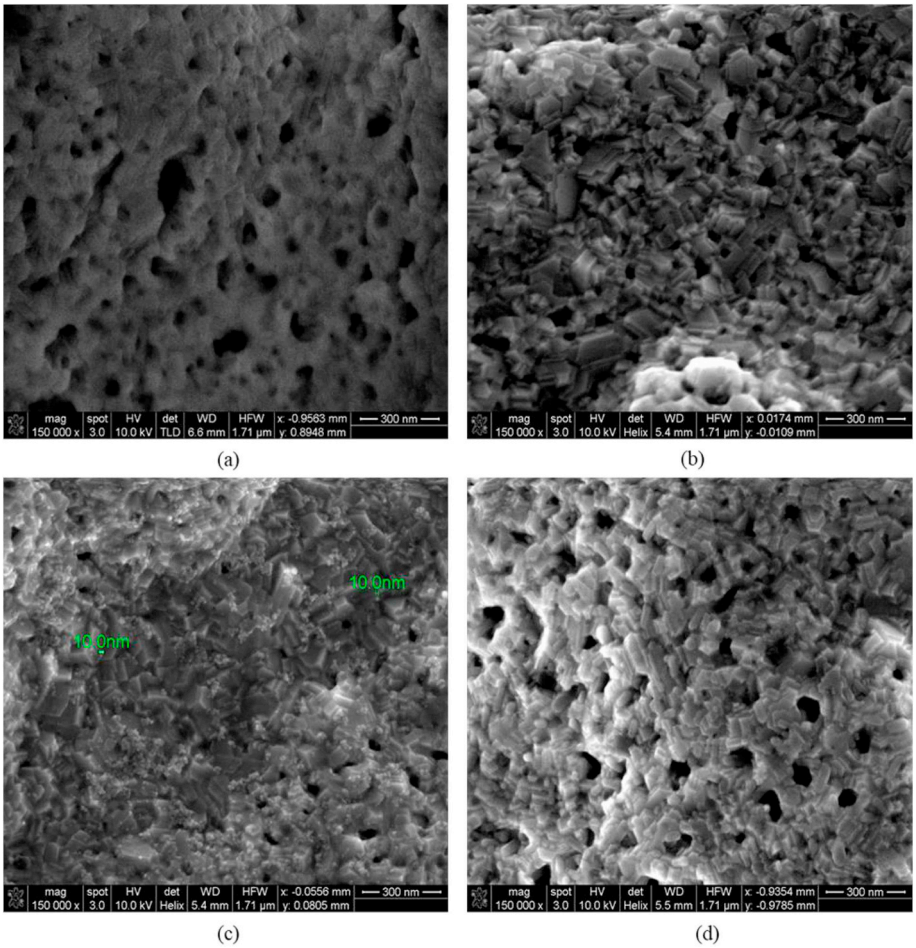

Fig. 1. SEM images of bare Gold (a); 16-AHT/Gold (b); mAb/16-AHT/Gold (c), and mAb-BSA/16-AHT/Gold (d). (For interpretation of the references to colour in this figure legend, the reader is referred to the Web version of this article.)

linkage occurs through a peptide bond that should, theoretically, not affect its bioactivity.

However, the biosensor efficiency was found to be enhanced when EDC alone was used [30]. We compared the use of EDC alone and the use of EDC along with NHS (data not shown). The results corroborated the previous idea, which is a reason why we adopted this method.

A 50 µL aliquot of the EDC-activated mAb antibodies was then incubated overnight at 4 °C. A final step consisting of the addition of PBS containing 1% bovine serum albumin (BSA) was carried out in order to block the non-specific binding sites on the sensing area.

2.5. Optimization of the antibody concentration under static conditions

In order to be able to minimize the final cost of the biosensor, we tested the anti-*Legionella* antibody at 3 different concentrations: 0.01, 0.05, and 0.1 mg/mL. These three concentrations were tested to detect *Legionella* in static mode as follows: 10 µL of the dilution containing *Legionella* at 10 CFU/mL were deposited on the pretreated area of the SPE and then left for 3 h of incubation at room temperature and finally rinsed with PBS solution and characterized electrochemically using CV and SWV. On the same biosensor, 10 µL of *Legionella* at 10^2 CFU/mL was added and the same procedure was performed, and so on, each time adding a 10-fold higher concentration of bacteria until *Legionella* at 10^8 CFU/mL was reached. This procedure was used to obtain a more reliable indication of the occurrence of sensor saturation.

As in our previous work regarding the detection of *Legionella* under static conditions [35], the sensor was incubated for 3 h [31] so that the bacterial cell capturing time could be considered to be long enough to assure a comparative results with the dynamic mode of detection. The sensor was kept in a sealed empty Petri dish to avoid surface dryness during the incubation.

2.6. Dynamic detection

The *Legionella* detection experiments under dynamic conditions were carried out in a glove box. The SPE was inserted into a microfluidic cell (volume of the cell: 8 µL; Input Diameter: 1 mm - Metrohm, France) linked to a cell inlet and connected to the tube containing the bacterial suspension (2 mL). Circulation was achieved using a peristaltic pump (Watson-Marlow, type 101 U/R) and the bacterial suspensions were recirculated 5 times at a maximum speed of 100 µL min^{-1}. The SPE electrode was then characterized electrochemically. The dilutions were tested using the same cumulative process described for the static mode.

2.7. Biosensing performance under dynamic conditions

In order to evaluate the efficiency of this mode of detection, 2 mL aliquots of the pre-circulated and the post-circulated contaminated samples were evaluated by culture: 500 µL of 10, 10^2, and 10^3 CFU/mL samples were plated on four BCYE plates (eight plates for each concentration). For each bacterial concentration, the initial suspension and the recirculated suspension (total volume of 2 mL for each one) were plated on BCYE agar supplemented with chloramphenicol and incubated at 37 °C for 72 h. All of the BCYE plates were observed under UV light at 366 nm to enumerate GFP-*L. pneumophila* colonies. Flow

cytometry assays (FCA) (Cube6, Sysmex) were also carried out to assess the physiological states of the bacteria: dead, alive, and 'viable but nonculturable' (VBNC) before and after fluid circulation. The quantification protocol was as described in our previous study [36]. Thus, 2 mL of 10^5 CFU/mL was processed for quantification using this technique.

3. Results and discussion

3.1. Validation of the surface modification: layer formation

The subsequent functionalization steps carried out on the bare gold electrode successively resulted in three modified surfaces: 16-AHT/Gold, mAb/16-AHT/Gold, and mAb-BSA/16-AHT/Gold. Each of these three modified surfaces was characterized by microscopic imaging techniques and by electrochemical measurements taking into account the responses obtained with the bare gold surface.

3.1.1. SEM and AFM characterization

3.1.1.1. SEM characterization. SEM imaging was carried out on the bare gold surface (Fig. 1a) and on each of the three subsequent modified surfaces (Fig. 1b, c, 1d). As can be seen in Fig. 1a, the surface topography of the typical gold electrode exhibited a high level of definition and homogeneity of the gold film. Compared to the SEM images of the bare gold surface, those obtained from the functionalized surfaces revealed various new 'geometric shapes' that clearly indicated effective immobilization of the corresponding molecules (16-AHT). In terms of the first functionalization step (Fig. 1b), the corresponding geometric shapes appeared to be quite smooth and the shapes had a narrow size range. Furthermore, this range did not change over the entire surface. Such forms could be the result of organized self-assembled monolayers of 16-AHT (Fig. 1b). A similar result was previously reported by Heimel et al. [37] using the simulated adsorption geometry for 4′-substituted-4-mercaptobiphenyls. These results suggest that the self-assembled molecules (SAM) can undergo a similar formation process. The SEM image of the antibody-modified surface (0.1 mg/mL) revealed grainy forms distributed homogeneously over the entire surface (Fig. 1c), suggesting successful mAb linkage to the 16-AHT modified surface. As can be seen in Fig. 1d, the SEM image of the BSA-treated surface (mAb-BSA/16-AHT/Gold) revealed the presence of more irregular shapes that were between 20 and 50 nm in size. This could be attributed to the adsorption of BSA on non-specific mAb binding areas. Our results, and those reported by others [38,39], confirm the successful use of SEM imaging to characterize modified surfaces during biosensor fabrication.

3.1.1.2. AFM characterization. The topography of the bare gold surface and each of the three modified surfaces was analysed using atomic force microscopy (AFM). The roughness parameter was evaluated as the average root mean square roughness (RMS) based on five measurements performed at five different locations (2 × 2 μm^2) on the surface. The roughness of the bare gold surface differed from that obtained for the modified gold surface, suggesting the formation of layers of film on the gold surface. Depending on the functionalization step, the analysed surface exhibited a reduced RMS roughness with a substantial standard deviation (Table 1). These results could be explained by both the surface heterogeneity induced by the chemical modification and the manufacturing process of the screen-printing technology of gold particles suspended in an ink on a ceramic substrate [40]. Yet, ultra-flat surfaces could be obtained using the pressure forming template stripping fabrication technique (0.35 ± 0.05 nm RMS roughness), as previously reported [41]. Overall, the generation of rough surfaces is one of the most convenient and effective ways to improve sensing signals [42]. Following the first step of modification (16-AHT) of the gold substrate, the standard deviation decreased, suggesting good coverage of the modified surface. According to Love et al. [43], SAMs can be fabricated into patterns in the plane of a surface with dimensions ranging from 10 to 100 nm, thus resulting in the formation of a geometric shape through the formation of an assembled monolayer. For the antibody modified surface, the slight decrease in the standard deviation could be the result of the immobilization of the antibody molecules. The addition of BSA appears to indicate better coverage of the surface, which could be due to the adsorption of BSA molecules at different angles, as previously reported [41].

Table 1
RMS value evaluation based on the AFM results (2 × 2 μm^2).

Surface	RMS value ± SD (nm)
Bare gold	164 ± 75
16-AHT/Gold	149 ± 55
mAb/16-AHT/Gold	148 ± 73
mAb-BSA/16-AHT/Gold	131 ± 54

3.1.2. Electrochemical characterization (SWV and CV)

Electrochemical measurements remain the most effective method for surface analysis during the fabrication process and the performance of the biosensor. In our study, the electrochemical behaviour of the modified surface was investigated using square-wave voltammetry (SWV) and cyclic voltammetry (CV) of the bare gold electrode and the three subsequent modifications with 16-AHT, mAb, and BSA, respectively.

As can be seen in Fig. 2, the peak current in SWV of the bare gold electrode was lower for each of the subsequent modified surfaces, suggesting immobilization of probe molecules. The highest current response occurred for the gold electrode (red curve). The peak current decreased substantially after treatment of the gold surface with aminothiol molecules (blue curve). The subsequent modification of the 16-AHT/Gold surface with antibody molecules was associated with a further decrease in the corresponding peak current of SWV (green curve), whereas no peak current change was observed after BSA treatment.

The observed decrease of the peak potentials by SWV after each of the two subsequent functionalization steps of the bare gold electrode could be related to a restricted mass transfer of redox species. This could be due to the molecular length of the covalently linked aminothiol and mAb molecules [44,45].

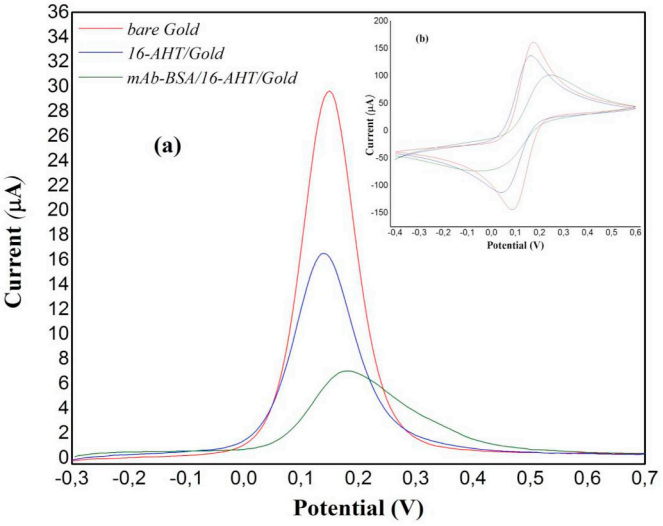

Fig. 2. Square-wave voltammetry (a) and cyclic voltammetry (b) of the modified electrode of bare Gold (red), 16-AHT/Gold (blue), and mAb-BSA/16-AHT/Gold (green). (For interpretation of the references to colour in this figure legend, the reader is referred to the Web version of this article.)

Furthermore, the reduction of the amplitudes of the current peaks recorded after the functionalization steps was associated with a slight change in the peak potential location. The peak current of the gold electrode was located at + 0.15 V whereas the peak current of the aminothiol-treated electrode was shifted to +0.13 V. This slight potential shift of the peak current towards a lower voltage for the 16-AHT-modified surface could be related to the presence of a positive electrostatic charge around the H_2N-terminated thiol-linked molecules. Indeed, at the pH that was used (a pH of 7.4), and taking into account a pKa of 10.6 for the NH_3+/NH_2 couple [46], the protonated form of the base predominated (NH_3+). Moreover, the current peak for the treated surface with mAbs underwent a positive shift relative to that obtained following the first functionalization step. The corresponding peak appeared at + 0.18 V. This additional shift could be the result of the negative charge of the mAbs carboxyl groups at pH = 7.4. The negative charges introduced after mAb treatment would neutralize the positive charges of the amino functional groups. This could explain the shift of the current peak to a higher voltage following the second step of the functionalization of the biosensor. Similar results have been reported based on electrochemical impedance spectroscopy [18]. The changes noted with SWV were confirmed by cyclic voltammetry. The same variation was found in the characterized signals as discussed for the SWV results. Of note, there was a greater decrease of the peak current with SWV compared to CV. This could be due to the sensitivity of the SWV technique. Indeed, SWV measures both the forward and the reverse current, while only the forward current is measured in CV [47].

All of these microscopic and electrochemical measurements suggest that the functionalization steps during the biosensor fabrication were successful. These data are in agreement with the results of the immunofluorescence experiment, which was carried out to make sure that the bioreceptor recognition sites were still accessible after the addition of BSA (using an Alexa Fluor 555 antibody, data not shown).

3.2. Antibody concentration optimization under static conditions

The aim of this part of the study was to estimate the lowest antibody concentration that would still ensure a linear electrochemical response, under static conditions, for bacterial suspensions ranging from 10 to 10^8 CFU/mL (as described in Section 2.4). Thus, three antibody concentrations of 0.01 mg/mL, 0.05 mg/mL, and 0.1 mg/mL were successively investigated.

The biosensor current signals needed for this study were, $I_{\text{mAb-BSA}}$ and $I_{\text{detection}}$, which were the recorded signals without bacteria and the bacterial concentrations, respectively. These recorded signals permitted us to calculate the ΔI/I as $[I_{(\text{mAb-BSA})} - I_{(\text{detection})}]/I_{(\text{mAb-BSA})}$. For each of the three antibody concentrations, a plot of the ΔI/I values versus the logarithm of the *Legionella* concentration is represented in Fig. 3.

As expected, there was a decrease in $I_{\text{detection}}$ due to bacterial capture, and thus an increase in the ΔI/I values as the bacterial concentration increased. The observed increase in the ΔI/I values could be attributed to the immobilization of bacterial cells, which acted as a barrier to electron transfer reactions on the biosensing surface. Such an impediment of the electron transfer kinetics on the electrode surface has been shown to occur during the formation of antibody/antigen complexes [45,48]. In order to confirm the immobilization of captured GFP-*L. pneumophila*, CLSM was performed. As shown in Fig. 3d, the images obtained indicate a homogeneous distribution of the captured bacterial cells at an antibody concentration of 0.1 mg/mL.

As can be seen in Fig. 3a and b, the ΔI/I values corresponding to antibody concentrations of 0.01 and 0.05 mg/mL did not increase in a linear manner with a *Legionella* concentration range from 10 to 10^8 CFU/mL. A saturation phenomenon was observed at these two antibody concentrations as the number of *Legionella* increased. By contrast, at an antibody concentration of 0.1 mg/mL (Fig. 3c), a linear increase in ΔI/I values was observed over a bacterial concentration range from 10 to 10^8 CFU/mL (R^2 = 0.975).

Therefore, under static conditions, the electrochemical biosensor functionalized with an antibody concentration of 0.1 mg/mL exhibited a wide linear response that ranged from 10 to 10^8 CFU/mL.

At an antibody concentration of 0.1 mg/mL, the limit of detection (LOD) was calculated to be 3 × SD (SD: standard deviation, n = 3) obtained from three measurements taken in the absence of bacteria. Three peak currents were recorded in the absence of *Legionella*, with values of 7.22 (I_1), 7.02 (I_2), and 5.9 μA (I_3), with a mean value of 6.72 μA (I_0). Each of these three values (I_1, I_2, and I_3) was then used to obtain the corresponding immunosensor response in the absence of bacteria evaluated as $|I_0–I|/I_0$. The values for the three responses obtained were: 0.075, 0.044, and 0.122, with a mean value of 0.08 and an SD value of 0.04. Therefore, the LOD was calculated to be 3 × SD, thus yielding a value of 0.12 with regard to the immunoresponse. The corresponding LOD value expressed in CFU/mL was then obtained from the calibration curve (Fig. 3c), yielding a value of ~10 CFU/mL. This LOD value was expected since the immunosensor responses varied linearly with the logarithmic value of the bacterial concentration over eight orders of magnitude (Fig. 3c), which included 10 CFU/mL. This LOD value is at least one order of magnitude lower than the values reported to date for the detection of *Legionella pneumophila* using various other biosensing devices. Compared to the previously published works discussed in the Introduction, our immunosensor appears to be the best device to detect *Legionella pneumophila* at 10 CFU/mL. Moreover, our method has the advantage of a relatively rapid analysis time (180 min), in addition to being portable, easy to operate, and relatively inexpensive compared to the other available technologies. Despite the excellent LOD value that we obtained and these advantages, this detection limit remains quite high compared to the reference levels for cooling towers (< 100 CFU/L) [49] and thus needs to be improved. Another hurdle to be overcome is that this LOD is subject to the weakness of the corresponding response. As described above, the blank assay was associated with a biosensing response of $[\Delta I/I]_{\text{Blank}} = 0.08 \pm 0.04$. Otherwise, the immunosensor response with *Legionella* at 10 CFU/mL ($[\Delta I/I]_{10\ \text{CFU/mL}}$), obtained as the mean of three simultaneously measurements, was 0.08 ± 0.08. Thus, both of the $[\Delta I/I]_{\text{Blank}}$ and $[\Delta I/I]_{10\ \text{CFU/mL}}$ responses were nearly the same.

This result suggests that 10 CFU/mL corresponds to the limit of detection of *Legionella* under static conditions, and this is in agreement with the obtained LOD (3 × SD). Nevertheless, due to the weakness of the response value and the relatively high SD, it would not be easy to detect 10 CFU/mL every time. Thus, increasing the response value of 10 CFU/mL by changing the detection conditions could be of great interest. Such an improvement would result in a more efficient quantification of 10 CFU/mL.

3.3. Performance of the dynamic biosensor

3.3.1. Electrochemical characterization

The biosensor described above was used to perform electrochemical measurements to detect and quantify *Legionella* present in circulating solutions (dynamic conditions). The aim was to achieve a faster response time and amplified signal sensing compared to measurements performed under static conditions as discussed previously.

The biosensor was coupled to the microfluidic system as described in Section 2.6. The biosensor measurements were performed under dynamic conditions with an antibody concentration of 0.1 mg/mL. A plot of ΔI/I values vs. the logarithm of a *Legionella* concentration ranging from 10 to 10^6 CFU/mL is shown in Fig. 4 (red curve). It can be seen that, compared to the sensor performance under static conditions (blue curve), the performance under dynamic conditions (red curve) indicates an amplified biosensing response. Furthermore, a linear increase in the ΔI/I values was only observed up to 10^3 CFU/mL. Between 10^3 CFU/mL and 10^6 CFU/mL the representative curve trended downward and tended to plateau, whereas the ΔI/I values measured under static conditions revealed a linear increase over the entire

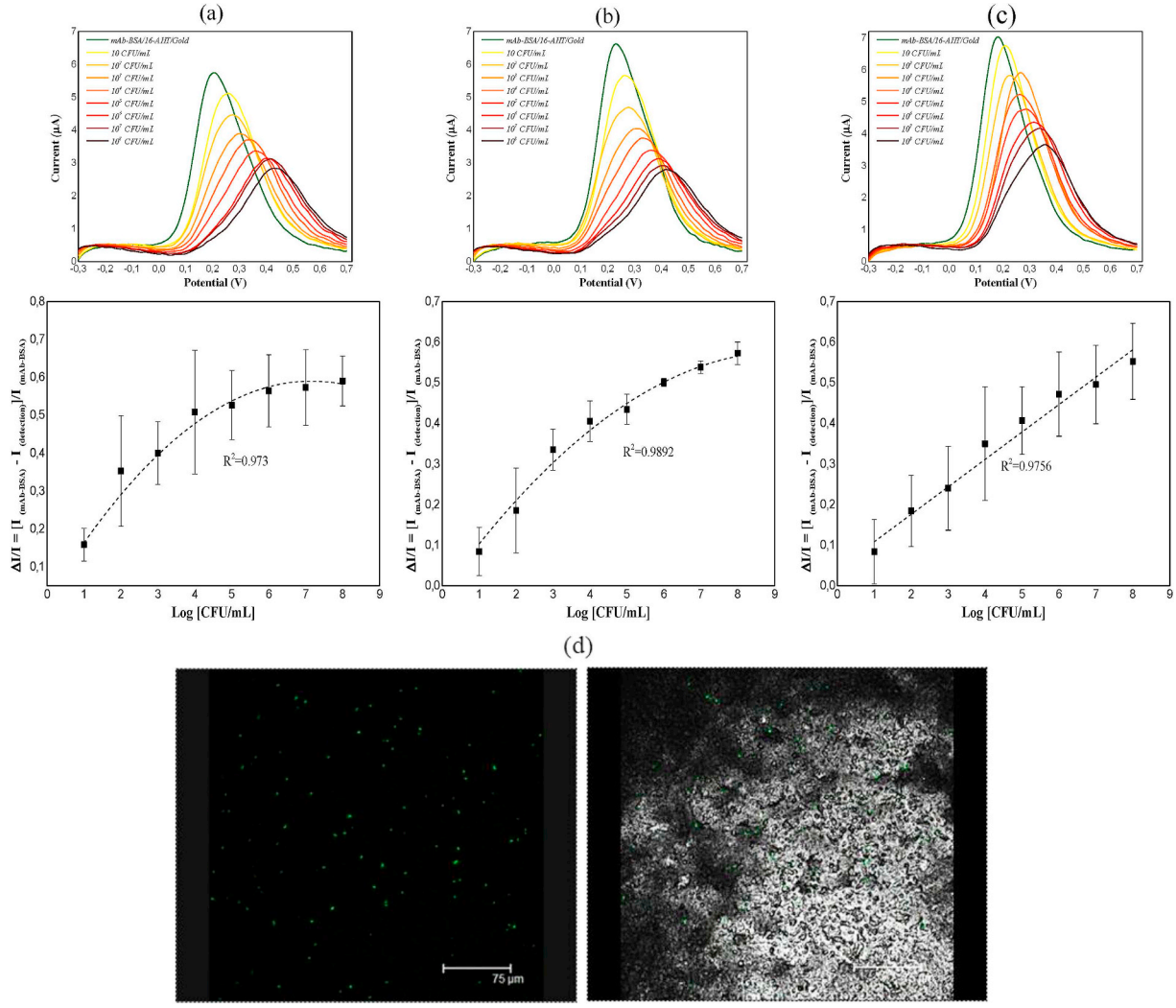

Fig. 3. SWV net currents and sensor performance for antibody concentrations of 0.01 mg/mL (a), 0.05 mg/mL (b), and 0.1 mg/mL (c) under static conditions. A CLSM image of captured GFP-L. pneumophila (left) and a CLSM image of captured GFP-L. pneumophila with reflectance mode (right) using an antibody concentration of 0.1 mg/mL (d).

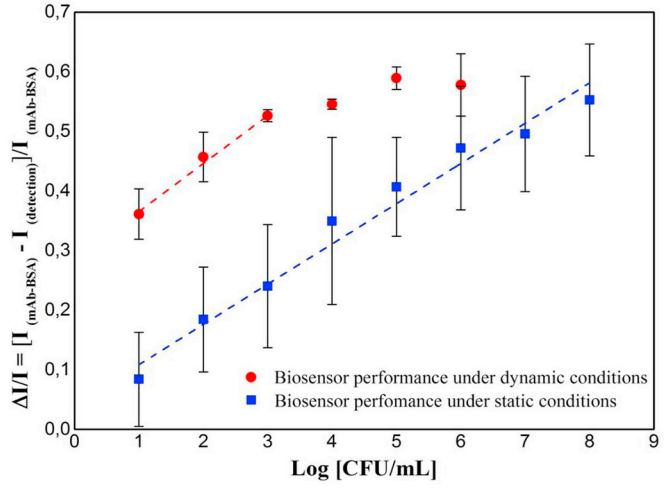

Fig. 4. Sensor performance: performance comparison between dynamic conditions (red curve) and static conditions (blue curve). (For interpretation of the references to colour in this figure legend, the reader is referred to the Web version of this article.)

$10–10^8$ CFU/mL bacterial concentration range. This finding illustrates the precocious appearance of a saturation phenomenon when the biosensor was used under dynamic conditions. Moreover, as can be seen in Fig. 4, the linear part of the curve established under dynamic conditions (R^2 = 0.991) was almost parallel to the linear representation obtained under static conditions. Considering that biosensor sensitivity is defined as the slope of the linear part of the calibration curve, our results suggest that the sensitivity of the biosensor under dynamic conditions remains almost the same as the sensitivity observed under static conditions. Circulation of each of the three bacterial concentrations (10, 10^2, and 10^3 CFU/mL) led to a nearly 4.5-fold increase in the ΔI/I values relative to the ΔI/I values obtained under static conditions., namely $[\Delta I/I]_{10\ CFU/mL} = 0.361 \pm 0.04$. The enhancement of the immunosensing response by the use of this microfluidic system suggests that it should be possible to use this biosensor under dynamic conditions to quantify *Legionella* at very low concentrations ranging from 10 to 10^3 CFU/mL. Due to the 4.5-fold increase in the immunosensing response achieved with circulation, a bacterial concentration of 10 CFU/mL can more readily be detected under dynamic conditions. In light of this, our method based on the use of circulating bacteria appears to be more suitable for quantification of *Legionella pneumophila* at a concentration of 10 CFU/mL. In addition, it seems likely that the detection limit should be significantly lower compared to the LOD

Table 2
Post-quantitative assessment of Legionella in recirculated artificially contaminated samples by culture.

Theoretical concentrations based on OD measurements	Enumerated colonies by culture: based on the number of the non-stressed (live) bacteria		
	Before circulation (CFU/mL)	After circulation (CFU/mL)	Percentage decrease
10	15	5	67%
10^2	96	45	53%
10^3	945	601	36%

obtained under static conditions. Furthermore, the incubation time with the bacteria was reduced from 180 min under static conditions to 100 min under dynamic conditions. The enhancement in the immunosensing response under dynamic conditions may be attributed to the increase in the number of cells captured by recirculation of the *Legionella* samples. This is, on the one hand, directly linked to a higher probability of contact between the bacteria cells and the functionalized surface and, on the other hand, it explains the occurrence of a precocious saturation phenomenon under dynamic conditions.

Moreover, linearity was not sought for bacterial samples at high concentrations since the aim of this study was to detect and quantify *Legionella* at very low concentrations. In France, the law of the decree of February 1st, 2010 [50] specifies that target values of 10^3 CFU/L in public entities and 10 CFU/L in healthcare institutions should be used for *Legionella* risk assessment.

3.3.2. Physiological state of Legionella under dynamic conditions

In order to evaluate the impact of dynamic conditions on the physiological state of *Legionella*, culture and flow cytometry measurements were performed.

FCA (as described in Section 2.7), was applied to a bacterial concentration of 10^5 CFU/mL. The percentage of dead cells before and after sample circulation was almost the same: 27% for the bacterial cell input (the precirculated aqueous sample) and 29% after dynamic detection. Thus, these results indicate that the microfluidic system did not affect the viability of the *Legionella* cells under dynamic conditions. Moreover, similar to the results obtained by the culture method, the FCA results confirm, as in our previous study [18], that viable and culturable cells as well as viable but nonculturable cells were captured by the biosensor with the same degree of efficacy.

Table 2 presents the number of colonies for the three *Legionella* concentrations ranging from 10 to 10^3 CFU/mL. When performed with the precirculated aqueous samples, 15, 96, and 945 colonies were enumerated for the corresponding theoretical concentration of 10, 10^2, and 10^3 CFU/mL, respectively. For these three bacterial concentrations, the plates incubated with recirculated solutions had 5, 45, and 601 enumerated colonies, respectively. Thus, these results indicate a decrease in the number of enumerated colonies when the cultures were performed with recirculated solutions compared to cultures performed prior to circulation. Percentage-wise, these decreases were 67%, 53%, and 36%, respectively. The decrease in *Legionella* cells in the circulated solutions could result in more bacterial cells being captured, thereby leading to enhancement of the biosensing signals with regard to ΔI/I values.

As described above, a similar linear relationship was found between the ΔI/I values and the logarithm of the bacterial concentration ranging from 10 to 10^3 CFU/mL. Moreover, we found a linear relationship by plotting the percentage of captured cells and the logarithm of the corresponding concentrations (R^2 = 0.996). These two linear relationships suggest that the ΔI/I values were correlated to the percentage decrease in the number of colonies (R^2 = 0.977). Therefore, it can be assumed that the increase in ΔI/I values was due to the greater extent of *Legionella* capture under dynamic conditions.

4. Conclusion

An electrochemical method was developed by coupling a functionalized biosensor with a microfluidic cell for the detection of *Legionella pneumophila* sg1 in water samples. The main functionalization steps of the biosensor were performed by covalent linkage of a self-assembled monolayer of 16-amino-1-hexadecanethiol (16-AHT) onto a gold surface to immobilize an anti-*L. pneumophila* monoclonal antibody (mAb). Characterization by electrochemical methods and microscopic imaging techniques indicated immobilization of both the mAb and the targeted bacteria. Under static conditions, the biosensor exhibited a wide linear response range from 10 to 10^8 CFU/mL and a detection limit of 10 CFU/mL. Using a microfluidic system, a linear biosensing signal was obtained between 10 and 10^3 CFU/mL, with a response amplification by a factor of 4.5 compared to the results under static conditions. Thus, the observed enhancement of the biosensor response should result in a better detection limit: less than 10 CFU/mL. Therefore, the use of this combination for electrochemical detection of *Legionella* cells has several advantages such as sensitivity, good response amplification, an easy fabrication process, a faster method, real-time detection, and portability. There is hence ample potential to expand the application of this biosensor configuration to assess the risk of *Legionella* bacterial contamination in environmental water systems, and a real-time biosensing signal could be of practical value in this field, especially during epidemics.

CRediT authorship contribution statement

Ahlem Laribi: Conceptualization, Data curation, Formal analysis, Investigation, Methodology, Visualization, Writing - original draft, Writing - review & editing. **Séverine Allegra:** Formal analysis, Writing - original draft. **Mina Souiri:** Conceptualization. **Ridha Mzoughi:** Methodology, Writing - original draft. **Ali Othmane:** Project administration, Resources, Supervision, Validation. **Françoise Girardot:** Validation, Formal analysis, Writing - original draft, Writing - review & editing, Funding acquisition.

Declaration of competing interests

The authors declare that they have no known competing financial interests or personal relationships that could have appeared to influence the work reported in this paper.

Acknowledgments

The authors gratefully acknowledge financial support from La Région Auvergne Rhône Alpes - CMIRA program. A special thanks to the late Prof. Serge RIFFARD who played a key role in spearheading this work.

The authors also thank the laboratory team of the GIMAP and Hubert Curien (Saint-Étienne, France) for their technical assistance.

References

[1] L. Sharma, A. Losier, T. Tolbert, C.S. Dela Cruz, C.R. Marion, Atypical pneumonia, Clin. Chest Med. 38 (2017) 45–58, https://doi.org/10.1016/j.ccm.2016.11.011.
[2] K.L. Dooling, K.-A. Toews, L.A. Hicks, L.E. Garrison, B. Bachaus, S. Zansky, L.R. Carpenter, B. Schaffner, E. Parker, S. Petit, A. Thomas, S. Thomas, R. Mansmann, C. Morin, B. White, G.E. Langley, Active bacterial core surveillance for legionellosis — United States, 2011–2013, MMWR Morb. Mortal. Wkly. Rep. 64 (2015) 1190–1193, https://doi.org/10.15585/mmwr.mm6442a2.
[3] E.A. Soda, A.E. Barskey, P.P. Shah, S. Schrag, C.G. Whitney, M.J. Arduino, S.C. Reddy, J.M. Kunz, C.M. Hunter, B.H. Raphael, L.A. Cooley, Vital signs: health care–associated legionnaires' disease surveillance data from 20 states and a large metropolitan area — United States, 2015, MMWR Morb. Mortal. Wkly. Rep. 66

(2017) 584–589, https://doi.org/10.15585/mmwr.mm6622e1.
[4] C. Campese, Christine, C., 2018. Légionellose 2018 : point de situation au 9 juillet 2018. Christine Campese (christine.campese@santepubliquefrance.fr, Direction des maladies infectieuses. Unité des infections respiratoires et vaccination, Agence nationale de santé publique France 12 rue du Val d'Osne 94415 Saint-Maurice Cedex France – Standard +33 (0)1 41 79 67 00, (2018) https://www.srlf.org/wp-content/uploads/2018/07/Legionellose-bilan-2018-au-09-07-2018.pdf , Accessed date: July 2019.
[5] P. Borella, E. Guerrieri, I. Marchesi, M. Bondi, P. Messi, Water ecology of Legionella and protozoan: environmental and public health perspectives, Biotechnology Annual Review, Elsevier, 2005, pp. 355–380, , https://doi.org/10.1016/S1387-2656(05)11011-4.
[6] K.D. Beer, J.W. Gargano, V.A. Roberts, V.R. Hill, L.E. Garrison, P.K. Kutty, E.D. Hilborn, T.J. Wade, K.E. Fullerton, J.S. Yoder, Surveillance for waterborne disease outbreaks associated with drinking water - United States, 2011-2012, MMWR Morb. Mortal. Wkly. Rep. 64 (2015) 842–848.
[7] A. Mobed, B. Baradaran, M. de la Guardia, M. Agazadeh, M. Hasanzadeh, M.A. Rezaee, J. Mosafer, A. Mokhtarzadeh, M.R. Hamblin, Advances in detection of fastidious bacteria: from microscopic observation to molecular biosensors, TrAC Trends Anal. Chem. (Reference Ed.) 113 (2019) 157–171, https://doi.org/10.1016/j.trac.2019.02.012.
[8] L.T. Orkis, L.H. Harrison, K.J. Mertz, M.M. Brooks, K.J. Bibby, J.E. Stout, Environmental sources of community-acquired legionnaires' disease: a review, Int. J. Hyg Environ. Health 221 (2018) 764–774, https://doi.org/10.1016/j.ijheh.2018.04.013.
[9] T. Baldovin, A. Pierobon, C. Bertoncello, May car washing represent a risk for Legionella infection? Ann. Ig. Med. Preventiva Comunita (2018) 57–65, https://doi.org/10.7416/ai.2018.2196.
[10] J. Walker, The influence of climate change on waterborne disease and *Legionella* : a review, Perspect. Public Health 138 (2018) 282–286, https://doi.org/10.1177/1757913918791198.
[11] P. Delgado-Viscogliosi, T. Simonart, V. Parent, G. Marchand, M. Dobbelaere, E. Pierlot, V. Pierzo, F. Menard-Szczebara, E. Gaudard-Ferveur, K. Delabre, J.M. Delattre, Rapid method for enumeration of viable Legionella pneumophila and other Legionella spp. in water, Appl. Environ. Microbiol. 71 (2005) 4086–4096, https://doi.org/10.1128/AEM.71.7.4086-4096.2005.
[12] A.K.T. Kirschner, Determination of viable legionellae in engineered water systems: do we find what we are looking for? Water Res. 93 (2016) 276–288, https://doi.org/10.1016/j.watres.2016.02.016.
[13] L. Alleron, A. Khemiri, M. Koubar, C. Lacombe, L. Coquet, P. Cosette, T. Jouenne, J. Frere, VBNC Legionella pneumophila cells are still able to produce virulence proteins, Water Res. 47 (2013) 6606–6617, https://doi.org/10.1016/j.watres.2013.08.032.
[14] E. Dietersdorfer, A. Kirschner, B. Schrammel, A. Ohradanova-Repic, H. Stockinger, R. Sommer, J. Walochnik, S. Cervero-Aragó, Starved viable but non-culturable (VBNC) Legionella strains can infect and replicate in amoebae and human macrophages, Water Res. 141 (2018) 428–438, https://doi.org/10.1016/j.watres.2018.01.058.
[15] C.-W. Chang, Y.-H. Hwang, W.-Y. Cheng, C.-P. Chang, Effects of chlorination and heat disinfection on long-term starved Legionella pneumophila in warm water, J. Appl. Microbiol. 102 (2007) 1636–1644, https://doi.org/10.1111/j.1365-2672.2006.03195.x.
[16] S. Allegra, F. Grattard, F. Girardot, S. Riffard, B. Pozzetto, P. Berthelot, Longitudinal evaluation of the efficacy of heat treatment procedures against *Legionella* spp. in hospital water systems by using a flow cytometric assay, Appl. Environ. Microbiol. 77 (2011) 1268–1275, https://doi.org/10.1128/AEM.02225-10.
[17] H.-Y. Lin, Y.-C. Tsao, W.-H. Tsai, Y.-W. Yang, T.-R. Yan, B.-C. Sheu, Development and application of side-polished fiber immunosensor based on surface plasmon resonance for the detection of Legionella pneumophila with halogens light and 850nm-LED, Sens. Actuators Phys. 138 (2007) 299–305, https://doi.org/10.1016/j.sna.2007.05.015.
[18] D. Sboui, M. Souiri, S. Reynaud, S. Palle, M.B. Ismail, T. Epalle, R. Mzoughi, F. Girardot, S. Allegra, S. Riffard, A. Othmane, Characterisation of electrochemical immunosensor for detection of viable not-culturable forms of Legionellla pneumophila in water samples, Chem. Pap. 69 (2015), https://doi.org/10.1515/chempap-2015-0170.
[19] N. Li, A. Brahmendra, A.J. Veloso, A. Prashar, X.R. Cheng, V.W.S. Hung, C. Guyard, M. Terebiznik, K. Kerman, Disposable immunochips for the detection of *Legionella pneumophila* using electrochemical impedance spectroscopy, Anal. Chem. 84 (2012) 3485–3488, https://doi.org/10.1021/ac3003227.
[20] K.F. Lei, P.H.M. Leung, Microelectrode array biosensor for the detection of Legionella pneumophila, Microelectron. Eng. 91 (2012) 174–177, https://doi.org/10.1016/j.mee.2011.10.002.
[21] M. Martín, P. Salazar, C. Jiménez, M. Lecuona, M.J. Ramos, J. Ode, J. Alcoba, R. Roche, R. Villalonga, S. Campuzano, J.M. Pingarrón, J.L. González-Mora, Rapid Legionella pneumophila determination based on a disposable core–shell Fe 3 O 4 @ poly(dopamine) magnetic nanoparticles immunoplatform, Anal. Chim. Acta 887 (2015) 51–58, https://doi.org/10.1016/j.aca.2015.05.048.
[22] D.L. Enrico, M.G. Manera, G. Montagna, F. Cimaglia, M. Chiesa, P. Poltronieri, A. Santino, R. Rella, SPR based immunosensor for detection of Legionella pneumophila in water samples, Optic Commun. 294 (2013) 420–426, https://doi.org/10.1016/j.optcom.2012.12.064.
[23] A.M. Foudeh, D. Brassard, M. Tabrizian, T. Veres, Rapid and multiplex detection of Legionella's RNA using digital microfluidics, Lab Chip 15 (2015) 1609–1618, https://doi.org/10.1039/C4LC01468E.
[24] M.R. Aziziyan, W.M. Hassen, H. Sharma, E. Shirzaei Sani, N. Annabi, E.H. Frost, J.J. Dubowski, Sodium dodecyl sulfate decorated Legionella pneumophila for enhanced detection with a GaAs/AlGaAs nanoheterostructure biosensor, Sensor. Actuator. B Chem. 304 (2020) 127007, https://doi.org/10.1016/j.snb.2019.127007.
[25] A. Mobed, M. Hasanzadeh, P. Babaie, M. Agazadeh, A. Mokhtarzadeh, M.A. Rezaee, DNA-based bioassay of legionella pneumonia pathogen using gold nanostructure: a new platform for diagnosis of legionellosis, Int. J. Biol. Macromol. 128 (2019) 692–699, https://doi.org/10.1016/j.ijbiomac.2019.01.125.
[26] V. Rai, Y.T. Nyine, H.C. Hapuarachchi, H.M. Yap, L.C. Ng, C.-S. Toh, Electrochemically amplified molecular beacon biosensor for ultrasensitive DNA sequence-specific detection of Legionella sp, Biosens. Bioelectron. 32 (2012) 133–140, https://doi.org/10.1016/j.bios.2011.11.046.
[27] P. Mustapha, T. Epalle, S. Allegra, F. Girardot, O. Garraud, S. Riffard, Monitoring of Legionella pneumophila viability after chlorine dioxide treatment using flow cytometry, Res. Microbiol. 166 (2015) 215–219, https://doi.org/10.1016/j.resmic.2015.01.004.
[28] S.K. Vashist, C.K. Dixit, B.D. MacCraith, R. O'Kennedy, Effect of antibody immobilization strategies on the analytical performance of a surface plasmon resonance-based immunoassay, Analyst 136 (2011) 4431, https://doi.org/10.1039/c1an15325k.
[29] S.K. Vashist, E. Marion Schneider, E. Lam, S. Hrapovic, J.H.T. Luong, One-step antibody immobilization-based rapid and highly-sensitive sandwich ELISA procedure for potential in vitro diagnostics, Sci. Rep. 4 (2015), https://doi.org/10.1038/srep04407.
[30] S.K. Vashist, Comparison of 1-ethyl-3-(3-dimethylaminopropyl) carbodiimide based strategies to crosslink antibodies on amine-functionalized platforms for immunodiagnostic applications, Diagnostics 2 (2012) 23–33, https://doi.org/10.3390/diagnostics2030023.
[31] M. Ben Ismail, F. Carreiras, R. Agniel, D. Mili, D. Sboui, N. Zanina, A. Othmane, Application of APTES-Anti-E-cadherin film for early cancer monitoring, Colloids Surf. B Biointerfaces 146 (2016) 550–557, https://doi.org/10.1016/j.colsurfb.2016.06.048.
[32] Y.-N. Chou, F. Sun, H.-C. Hung, P. Jain, A. Sinclair, P. Zhang, T. Bai, Y. Chang, T.-C. Wen, Q. Yu, S. Jiang, Ultra-low fouling and high antibody loading zwitterionic hydrogel coatings for sensing and detection in complex media, Acta Biomater. 40 (2016) 31–37, https://doi.org/10.1016/j.actbio.2016.04.023.
[33] R. Raghav, S. Srivastava, Immobilization strategy for enhancing sensitivity of immunosensors: L -Asparagine–AuNPs as a promising alternative of EDC–NHS activated citrate–AuNPs for antibody immobilization, Biosens. Bioelectron. 78 (2016) 396–403, https://doi.org/10.1016/j.bios.2015.11.066.
[34] C.K. Dixit, S.K. Vashist, B.D. MacCraith, R. O'Kennedy, Multisubstrate-compatible ELISA procedures for rapid and high-sensitivity immunoassays, Nat. Protoc. 6 (2011) 439–445, https://doi.org/10.1038/nprot.2011.304.
[35] M. Souiri, N. Blel, D. Sboui, L. Mhamdi, T. Epalle, R. Mzoughi, S. Riffard, A. Othmane, AFM, CLSM and EIS characterization of the immobilization of antibodies on indium–tin oxide electrode and their capture of Legionella pneumophila, Talanta 118 (2014) 224–230, https://doi.org/10.1016/j.talanta.2013.09.049.
[36] S. Allegra, F. Berger, P. Berthelot, F. Grattard, B. Pozzetto, S. Riffard, Use of flow cytometry to monitor Legionella viability, Appl. Environ. Microbiol. 74 (2008) 7813–7816, https://doi.org/10.1128/AEM.01364-08.
[37] G. Heimel, L. Romaner, J.-L. Brédas, E. Zojer, Interface energetics and level alignment at covalent metal-molecule junctions: π-conjugated thiols on gold, Phys. Rev. Lett. 96 (2006), https://doi.org/10.1103/PhysRevLett.96.196806.
[38] N. Mathebe, Electrochemistry and scanning electron microscopy of polyaniline/peroxidase-based biosensor, Talanta 64 (2004) 115–120, https://doi.org/10.1016/j.talanta.2003.11.050.
[39] C. Zhang, J. Lou, W. Tu, J. Bao, Z. Dai, Ultrasensitive electrochemical biosensing for DNA using quantum dots combined with restriction endonuclease, Analyst 140 (2015) 506–511, https://doi.org/10.1039/C4AN01284D.
[40] A. Butterworth, E. Blues, P. Williamson, M. Cardona, L. Gray, D.K. Corrigan, SAM composition and electrode roughness affect performance of a DNA biosensor for antibiotic resistance, Biosensors 9 (2019) 22, https://doi.org/10.3390/bios9010022.
[41] J.A. Rubio-Lara, F. Bergler, S.J. Attwood, J.M. Edwardson, M.E. Welland, Ultraflat gold QCM electrodes fabricated with pressure-forming template stripping for protein studies at the nanoscale, Langmuir (2019), https://doi.org/10.1021/acs.langmuir.8b03782.
[42] Y. Gao, S. Sun, S.-Q. Shi, F. Ciucci, T.-Y. Zhang, On-chip suspended gold nanowire electrode with a rough surface: fabrication and electrochemical properties, Electrochim. Acta 304 (2019) 20–29, https://doi.org/10.1016/j.electacta.2019.02.106.
[43] J.C. Love, L.A. Estroff, J.K. Kriebel, R.G. Nuzzo, G.M. Whitesides, Self-assembled monolayers of thiolates on metals as a form of nanotechnology, Chem. Rev. 105 (2005) 1103–1170, https://doi.org/10.1021/cr0300789.
[44] F. Chen, X. Li, J. Hihath, Z. Huang, N. Tao, Effect of anchoring groups on single-molecule conductance: comparative study of thiol-, amine-, and carboxylic-acid-terminated molecules, J. Am. Chem. Soc. 128 (2006) 15874–15881, https://doi.org/10.1021/ja065864k.
[45] X. Zhang, G. Shen, S. Sun, Y. Shen, C. Zhang, A. Xiao, Direct immobilization of antibodies on dialdehyde cellulose film for convenient construction of an electrochemical immunosensor, Sensor. Actuator. B Chem. 200 (2014) 304–309, https://doi.org/10.1016/j.snb.2014.04.030.
[46] J.C. Kromann, F. Larsen, H. Moustafa, J.H. Jensen, Prediction of pKa values using the PM6 semiempirical method, PeerJ 4 (2016) e2335, https://doi.org/10.7717/peerj.2335.
[47] P.K. Brahman, N. Pandey, J.V.S. Kumar, P. Somarouthu, S. Tiwari, K.S. Pitre, Highly

sensitive stripping voltammetric determination of a biomolecule, pyruvic acid in solubilized system and biological fluids, Arab. J. Chem. 9 (2016) S1897–S1904, https://doi.org/10.1016/j.arabjc.2014.02.003.

[48] Y. Yun, A. Bange, W.R. Heineman, H.B. Halsall, V.N. Shanov, Z. Dong, S. Pixley, M. Behbehani, A. Jazieh, Y. Tu, A nanotube array immunosensor for direct electrochemical detection of antigen–antibody binding, Sensor. Actuator. B Chem. 123 (2007) 177–182, https://doi.org/10.1016/j.snb.2006.08.014.

[49] R. Miranda-Castro, N. de-los-Santos-Álvarez, M.J. Lobo-Castañón, A.J. Miranda-Ordieres, P. Tuñón-Blanco, PCR-coupled electrochemical sensing of Legionella pneumophila, Biosens. Bioelectron. 24 (2009) 2390–2396, https://doi.org/10.1016/j.bios.2008.12.014.

[50] Arrêté du 1er février, Arrêté du 1er février 2010 relatif à la surveillance des légionelles dans les installations de production, de stockage et de distribution d'eau chaude sanitaire. NOR: SASP1002960A, n.d (2010) https://www.legifrance.gouv.fr/affichTexte.do?cidTexte=JORFTEXT000021795143&categorieLien=id , Accessed date: July 2019.